Monte Carlo calculated correction factors for primary standards of air kerma

D. W. O. Rogers[a] and Iwan Kawrakow
National Research Council of Canada, Ottawa K1A OR6, Canada

(Received 23 September 2002; accepted for publication 5 February 2003; published 21 March 2003)

Many laboratories with cavity chambers as primary standards for air kerma are considering using additional Monte Carlo calculated correction factors, in particular the correction for attenuation and scatter in the walls, K_{wall}, and possibly the correction for point of measurement, K_{an}. Standards labs also use Monte Carlo calculated Spencer-Attix stopping-power ratios for graphite to air. The purpose of this article is to investigate the sensitivity of these calculations to their details and to assign uncertainties to the calculated values. We also investigate the correction needed for the Canadian primary standard to account for a polystyrene insulator, K_{comp} and find that it is quite large (1.0046 ± 0.0017). The article shows that the values of correction factors are very robust and insensitive to most details of the calculations except the values of the underlying electron stopping powers which have a significant effect on the stopping-power ratio and on K_{comp}. The 1% uncertainties on the photon cross-sections have a negligible effect on these correction factors except for K_{comp}. As a result of these investigations, with no change in the stopping power data used, the Canadian primary standard of air kerma in a ^{60}Co beam needs to be increased by 0.54%.
[DOI: 10.1118/1.1563663]

I. INTRODUCTION

Primary standards for air kerma in a ^{60}Co beam have been the basis of clinical dosimetry for many years because dosimetry protocols such as the AAPM's TG-21[1] and the IAEA's TRS-277[2] are based on air-kerma calibration factors. Despite the fact that many dosimetry protocols are now based on absorbed-dose calibration factors (e.g., the AAPM's TG-51[3]), it is important to have accurate standards for air kerma, if only to allow meaningful comparisons between old and new dosimetry protocols. Primary standards for air kerma in a ^{60}Co beam are universally based on graphite-walled cavity ion chambers, albeit of many different shapes. The air kerma, K_{air}, is established at a point in the beam using

$$K_{air} = \frac{Q_{gas}}{m_{air}(1-\overline{g}_{air})} \left(\frac{W}{e}\right)_{air} \left(\overline{\frac{L}{\rho}}\right)_{air}^{wall} \left(\overline{\frac{\mu_{en}}{\rho}}\right)_{wall}^{air} \times K_h K_{wall} K_{an} K_{comp} K \quad (\mathrm{Gy}), \tag{1}$$

where Q_{gas} is the charge released in the air of mass m_{air}, $\overline{g}_{air}$ is the fraction of the energy of an electron lost in radiative events while slowing in air, $(W/e)_{air}$ is the energy lost in dry air per coulomb of charge released, $(\overline{L/\rho})_{air}^{wall}$ is the Spencer–Attix collision mass stopping-power ratio (spr) for the wall material to dry air, $(\overline{\mu_{en}/\rho})_{wall}^{air}$ is the ratio of mass energy absorption coefficients averaged over the spectrum for dry air to the wall material, K_h is the humidity correction factor[4] (taken as 1 in this study because all calculations are for dry air, but which in practice is needed since by convention the air kerma is always for dry air and measurements are made in humid air), K_{wall} corrects for the attenuation and scatter in the chamber wall, K_{an} corrects for the axial nonuniformity due to the point source nature of the beam instead of the photon beam being parallel, K_{comp} is a correction for the composite, i.e., nonuniform, nature of the wall material (if any) and K includes various corrections for other nonideal conditions (e.g., corrections for stems, central electrodes of different material from the wall, radial nonuniformity of the beam, etc., again, all unity in this study).

The definitions of some of the quantities in Eq. (1) are arbitrary and for clarity we will specify exactly what we mean. In this work we take the stopping-power ratio to be that for an incident parallel beam which experiences no scatter or attenuation in the chamber (see Sec. VIII A). The K_{wall} correction is traditionally taken as being for a point source at the appropriate distance from the realistic chamber (without a stem). This choice of definition is imposed since K_{wall} was originally based on measured data. Once this is defined, then K_{an} is defined (calculated) as

$$K_{an} = \frac{(D_{gas}K_{wall})_{realistic}^{parallel}}{(D_{gas}K_{wall})_{realistic}^{point}}, \tag{2}$$

where D_{gas} is the dose to the gas in the chamber and all quantities are calculated for the realistic model of the chamber. Similarly, the quantity K_{comp} is defined (calculated) as

$$K_{comp} = \frac{(D_{gas}K_{wall})_{graphite}^{parallel}}{(D_{gas}K_{wall})_{realistic}^{parallel}}. \tag{3}$$

These definitions are arbitrary but follow once the definition of K_{wall} is made. In other situations, other definitions are appropriate. For example, in a related work[5] the definition of K_{comp} for electron beam plane-parallel chambers must not include the ratio of wall attenuation factors because the goal was to equate the values of K_{comp} with the values of P_{wall}, the corresponding correction factor except in a water phantom and in this case the K_{wall} factors are conceptually inap-

propriate. This made the definition of K_{an} somewhat simpler because it too no longer required the K_{wall} factors, but the value of K_{wall} was then required to be for a parallel beam of photons incident on a homogeneous chamber. Computationally this is acceptable, but it means that the value of K_{wall} is, in principle, no longer measurable. As will be shown below, the fine points of these definitions have little practical impact, but they are needed for the sake of rigor.

If calculations were being done "*ab initio*" rather than using accepted values of $(\overline{\mu_{en}/\rho})^{air}_{wall}$, it might be more meaningful to write Eq. (1) as

$$K_{air}=\frac{Q_{gas}}{m_{air}(1-\overline{g}_{wall})}\left(\frac{W}{e}\right)_{air}\left(\overline{\frac{L}{\rho}}\right)^{wall}_{air}\left(\overline{\frac{\mu_{tr}}{\rho}}\right)^{air}_{wall} \times K_h K_{wall} K_{an} K_{comp} K \quad (\mathrm{Gy}), \tag{4}$$

since one often calculates the mass-energy transfer coefficient for a material, $(\overline{\mu_{tr}/\rho})_{mat}$, and deduces $(\overline{\mu_{en}/\rho})_{mat}$ by calculating $\overline{g}_{mat}$. This formulation emphasizes that we are only sensitive to the $\overline{g}_{wall}$ value [in Ref. 6, their related Eq. (2) has a typo-$(\overline{\mu_{en}/\rho})^{air}_{wall}$ should be $(\overline{\mu_{tr}/\rho})^{air}_{wall}$, which was used in the calculations].

Traditionally, national standards labs determined K_{wall} by adding additional wall thickness to ion chambers and linearly extrapolating the response versus wall thickness curve to determine the response for zero wall thickness (and also making a correction, K_{cep}, to account for the center of electron production). Starting in the mid 1980s, these factors were calculated using Monte Carlo codes and by 1990 it was found that, although the Monte Carlo codes could accurately reproduce the response versus wall thickness curves, the calculated values of K_{wall} were up to 1% different from those determined by linear extrapolation.[7] Based on a simple model, Bielajew[8] showed that the extrapolation was nonlinear for beams incident on a spherical chamber. Using his nonlinear extrapolation of the measured data led to reasonable agreement with the Monte Carlo calculations for the spherical chamber. At the same time, Bielajew[9] developed an analytic theory for K_{an} (the axial nonuniformity correction) to account for the fact that ion chambers are irradiated by a point source and not a parallel beam of photons [strictly, Bielajew's theory and Eq. (2) are for K_{pn}, the correction which includes the radial as well as axial nonuniformity introduced by the point source nature of the beam, but the radial nonuniformity is negligible at normal calibration distances]. This theory demonstrated that the amount of correction was very small for typical standards-laboratory ion chambers at about 100 cm from a source. Although this agreed with the procedures in most standards laboratories, there were several National Metrological Institutes (NMIs) for which this theory implied a substantial change.

A 1992 paper[10] showed that the combination of the above corrections based on Monte Carlo and analytic techniques would imply a 0.64% increase in the average air-kerma rate at several major standards laboratories. In a more recent and more detailed study using a different Monte Carlo code (EGSnrc[11] rather than EGS4[12]) and using direct calculations rather than using correlated scoring techniques to calculate K_{an}, the average increase in air-kerma rate for 16 primary standards for air kerma in a ^{60}Co beam was determined to be 0.8%.[13]

At the 2001 meeting of Section I of the BIPM's Consultative Committee on Ionizing Radiation (CCRI), there was a decision that NMIs would revisit their correction factors and consider using Monte Carlo calculated values. Since that time, several papers have appeared which lend experimental support to using calculated correction factors.[14–16] There is one particularly convincing experiment from the PTB which demonstrates that the linear extrapolation technique for determining K_{wall} is inappropriate.[17] We have undertaken a sensitivity study to investigate the uncertainties associated with these calculated values, and the sensitivity of the calculated values to such things as the Monte Carlo code used, the ^{60}Co spectrum used, the diameter of the ^{60}Co source, and the distance from the source. As well as investigating K_{wall}, we have undertaken to investigate the sensitivity of the calculated values of the other factors in Eq. (1), viz., K_{an}, K_{comp}, and $(\overline{L/\rho})^{graphite}_{air}$.

If most NMIs decide to switch to calculated values of K_{wall} and K_{an}, this leaves NRC in the situation that our primary standard for air kerma appears to be about 0.6% lower than the new world average, at least as predicted in Ref. 13. In another NRC study[6] it was noted that the plastic insulator in the 3C chamber actually had a much larger effect than determined in some technically difficult but hard to interpret experimental measurements (described in Ref. 18). We have investigated this issue further here.

II. MONTE CARLO CALCULATIONS

All calculations were carried out using the EGSnrc Monte Carlo system for radiation transport.[11,19] Unless otherwise noted, the calculations were done with the default settings of the code which includes modeling the Compton interaction as being from bound electrons, includes the effects of any atomic relaxation events and includes relativistic spin effects in the multiple scattering theory. It will be shown below that inclusion of these parameters has little effect on the calculated correction factors. The calculations made use of updated versions of the standard EGSnrc user-codes, viz., SPRRZnrc for calculating the stopping power ratios, $(\overline{L/\rho})^{wall}_{air}$ and CAVRZnrc for everything else. The Monte Carlo codes are both distributed with the EGSnrc system and described in detail in Ref. 20. Several new options have been added specifically for this study. These include a new coding of an off-axis point source routine, and a new routine to handle an isotropic source of finite radial dimension, rather than just a point source. The Monte Carlo simulations were done with various options turned off or on and these are described in more detail when used.

Although the majority of the calculations were done with EGSnrc, some calculations were carried out using the EGS4 Monte Carlo system[12] and some using the PRESTA algorithm.[21]

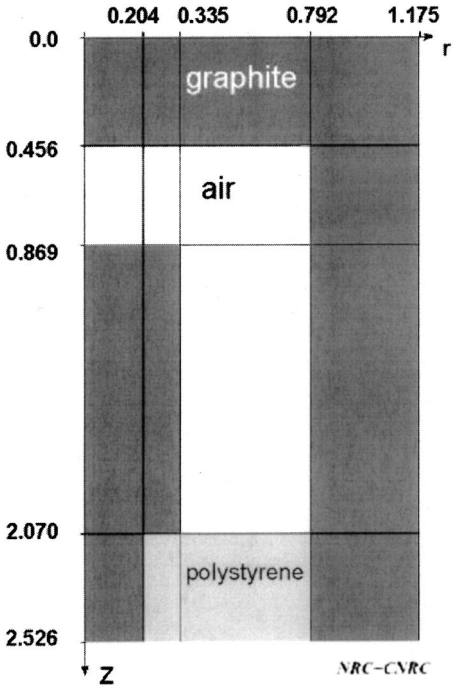

FIG. 1. Schematic of the 3C chamber as modeled for these calculations. The 3C chambers was built by W. H. Henry of NRC and has been used to establish Canada's primary standard for air kerma in a ^{60}Co beam for four decades. The chamber is rotationally symmetric about the z-axis. All dimensions are in cm. The density of the graphite is 1.66 g/cm^3.

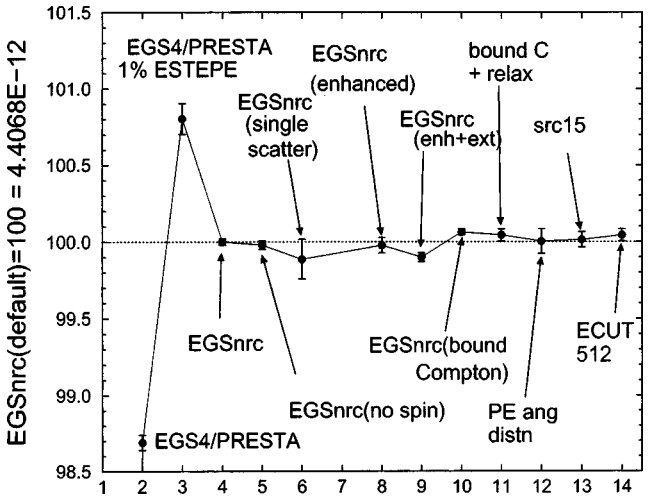

FIG. 2. Monte Carlo calculated values of 3C chamber response (D_{gas}/unit incident fluence) normalized to the default CAVRZnrc calculation with EGSnrc as 100 (4.4068E-12 Gy/cm^2). The first point (not shown) for default EGS4 is at 55%. All calculations are done with ECUT=521 keV except for case 14 which has ECUT=512 keV. The cases 1–14 are described in the text. There is no case 7.

II. A. Model of the 3C chamber

Figure 1 shows the 3C cavity ion chamber which has been the basis of the Canadian primary standard for air kerma for four decades. The density of the graphite is 1.66 g/cm^3 and this value is used in the calculations. The density effect used for the graphite stopping powers varied. In some studies, the ICRU density effect for a density of 1.70 g/cm^3 was used since it was available and close to the bulk density. However, electron stopping powers for graphite have recently been measured at NRC for electrons with energies between 7 and 30 MeV,[22,23] and there is a clear preference for using the grain density (2.26 g/cm^3) when calculating the density effect. In many calculations a density effect correction based on this value has been used.

A critical aspect of the 3C chamber is the large polystyrene insulator. It is more exposed to the cavity than the insulators in most cavity ion chambers used by NMIs.

III. VARIATION WITH DIFFERENT MONTE CARLO SIMULATIONS

III. A. Effect on calculated response

It has been suggested that one be cautious about using Monte Carlo calculated correction factors since the calculations have been done using only one Monte Carlo code, viz., EGS4. If this were true, it would constitute a valid criticism. However, the calculations have been done with what amounts to a wide variety of different electron transport algorithms, and with a variety of scoring and coding options. As shown below, despite giving a wide range of results for the ion chamber response, the different calculations all give the same results for K_{wall}, thereby demonstrating that the calculated values are robust.

Figure 2 shows the calculated relative response (D_{gas}/unit incident fluence) of NRC's 3C ion chamber. This figure demonstrates that the value of the response varies a great deal depending on which version of the code is used. The calculated response for the ion chamber using EGS4 in default mode is 45% lower than that calculated with the default EGSnrc calculation (which in this case has the relativistic spin option included but the binding effects in Compton scattering are not included and atomic relaxations are not modeled). Clearly the EGS4 algorithm and the EGSnrc transport algorithms are very different. Using EGS4 with the PRESTA algorithm, the result is about 1.5% less than the EGSnrc results and if the pathlength is further restricted to less than 1% energy loss per step, the calculated response is 0.8% greater than that of EGSnrc. The point is that these three calculations are done with very different transport algorithms, despite all being called EGS. As shown elsewhere,[24] only the EGSnrc calculations produce the correct response.

Within EGSnrc, there are many transport options which can be turned on or off. The figure shows that when relativistic spin effects are turned off, there is no change in the calculated response. If the condensed history approach is ignored and the entire calculation is done in single scattering mode, the calculated response does not change although the statistical uncertainties are much greater since the time per history increases dramatically. Although the calculated dose does not change, it is clear that the single scattering calculation constitutes a completely different algorithm. The results with binding effects taken into account show a small (about 0.05%) effect on the calculated response whereas the inclu-

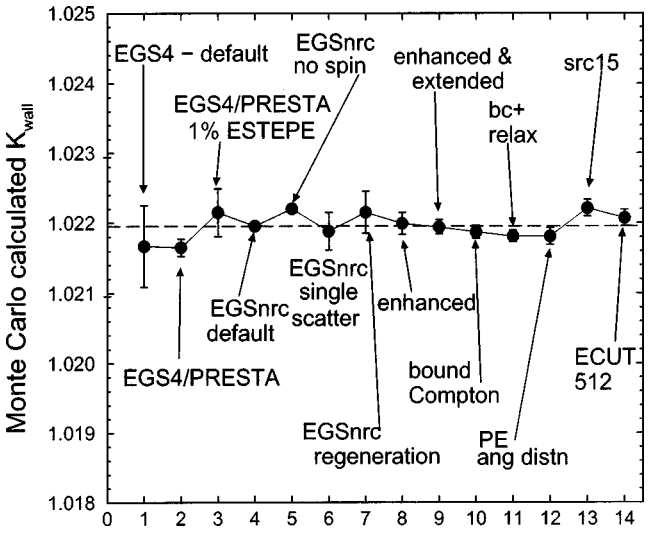

FIG. 3. Monte Carlo calculated values of K_{wall} for the 3C chamber based on very different electron transport algorithms.

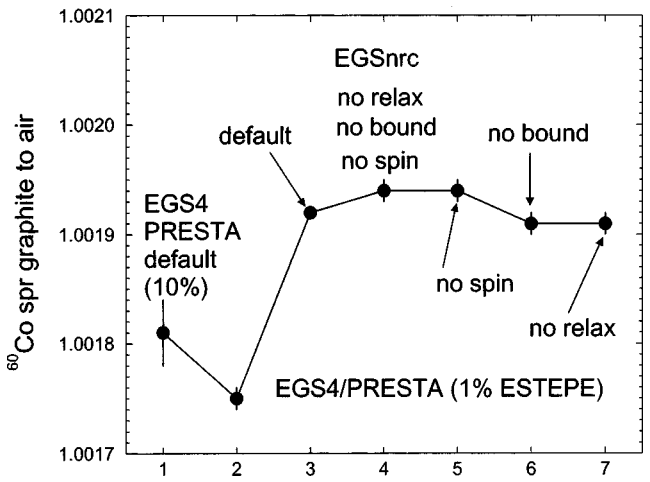

FIG. 4. Variation of ^{60}Co graphite to air stopping-power ratio (spr) when different versions of EGS are used. The default EGSnrc mode simulates bound compton interactions, relaxation of the atoms, and relativistic spin effects. Various runs with combinations of these turned off demonstrate that the calculated stopping-power ratio is insensitive to these details. All calculations are done for a phantom with 0.25 cm buildup. The EGSnrc results are done using SPRRZnrc with regeneration off to match the EGS4/PRESTA results (which are shown for two values of ESTEPE). The graphite density effect is for a density of 1.70 g/cm^3 and $\Delta = 10$ keV. Note that the *y*-axis extends over only 0.04% whereas most following figures cover 0.4%.

sion of relaxation or angular distributions of photo-electrons has no effect.

Most calculations in this study have been done with the low-energy limits for electron transport set at 10 keV. However, as case 14 shows, a reduction of the threshold (AE = ECUT) to 1 keV increases the response by a statistically insignificant 0.04%.

Any Monte Carlo simulation has other components which must be properly coded in order to produce accurate results, e.g., the routines for modeling the initial photons, the scoring routines, or the variance reduction routines. In most of the calculations reported above, the photons were forced to interact in the ion chamber, thereby improving the efficiency. However, an error in the forcing routines would not show up because the coding is common (although the fact that the absolute dose is calculated correctly means this is highly unlikely). Nonetheless, another, independent form of variance reduction was added to CAVRZnrc whereby the cross-section was enhanced rather than using the forcing routines. Calculations done with this option (result 8, Fig. 2) show no difference. Similarly, all the other routines use a complex, common routine for modeling a point source incident from an arbitrary angle. A new source routine (source 15) was implemented in CAVRZnrc and the results with this routine (result 13) were the same as the default case. Finally, a calculation was done using a version of the source routine with a finite source size rather than a point source, and here the response decreased by about 0.1% (result 9).

III. B. Effect of transport algorithm on calculated values of K_{wall}

Figure 3 presents the values of K_{wall} calculated in the same cases as shown in the previous figure for the response. Despite the 46% variation in calculated response in these calculations, the values of K_{wall} vary by no more than 0.04% from the calculations with the default EGSnrc. It is clear that the value of K_{wall} is not dependent on what code is used to calculate the result. The one remaining possibility is an error in the technique used by CAVRZnrc to calculate K_{wall}. This is a correlated technique in which the energy deposition from primaries is scored with and without being corrected for attenuation effects and the dose from scattered photons is scored separately.[7] Another independent approach to this calculation is to run it twice, once with the normal physics, and then with photon regeneration on, in which case a primary photon is regenerated after every interaction and all scattered photons are terminated. By definition, the ratio of the dose to gas in these two cases gives the value of K_{wall}, although much less efficiently than the correlated sampling method. Result 7 in Fig. 3 demonstrates that the results are the same within 0.02%, thus confirming the accuracy of the coding in the correlated scoring case.

The reduction of the electron transport threshold to 1 keV changes the result by 0.01%, which is not statistically significant.

III. C. Effect of EGS algorithm on stopping-power ratios

Figure 4 presents values of $(\overline{L}/\rho)_{air}^{graphite}$ calculated using SPRRZnrc and SPRRZ with a variety of electron transport algorithms. The calculations are all for a threshold value, Δ, of 10 keV. The figure demonstrates that the EGSnrc options used during the calculations of the stopping-power ratios have a negligible effect ($<0.002\%$) on the value. The difference between the EGSnrc and EGS4/PRESTA results are slightly larger but still negligible (up to nearly a 0.02% spread). These results in a small graphite cylinder do not necessarily generalize to all calculated stopping-power ratios since, e.g., turning spin on and off changes an electron beam

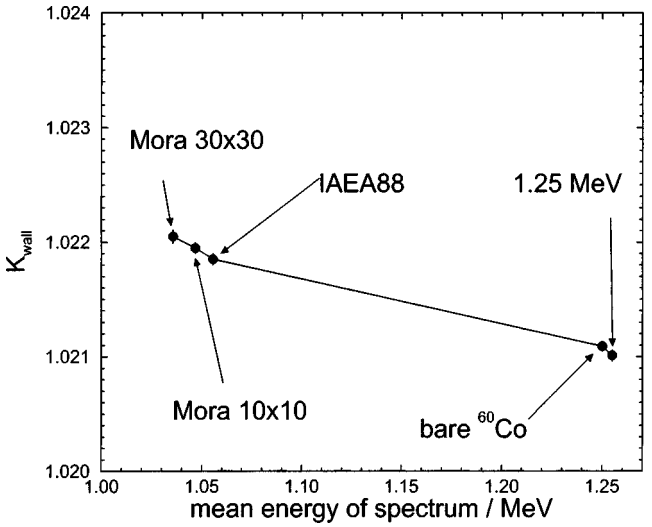

FIG. 5. Variation of K_{wall} value for the 3C chamber for the various spectra shown and described in the text.

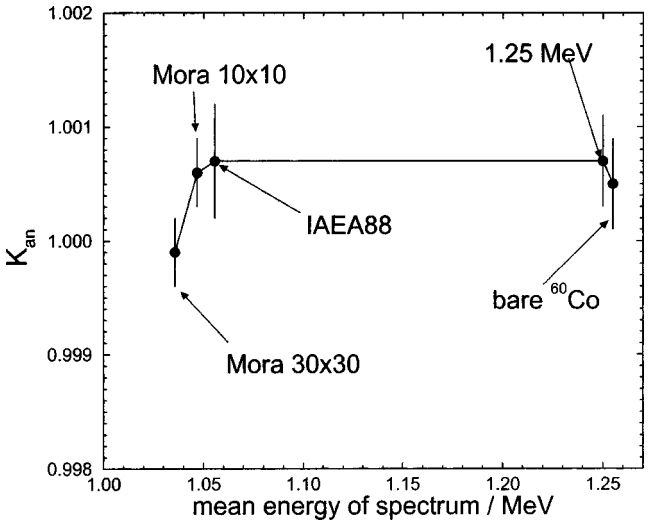

FIG. 6. Variation of K_{an} value for the 3C chamber for the various spectra shown. All values are for a point source at 100 cm.

depth-dose curve and can be expected to affect the stopping-power ratios as well (by up to about 0.1% as shown in Ref. 25).

IV. DEPENDENCE ON INCIDENT ^{60}Co SPECTRUM

The spectrum in different ^{60}Co beams will vary depending on the nature of the ^{60}Co source, the field size, etc. It is therefore valuable to study the effects of different photon spectra on the quantities of interest here.

To do this we have used five incident ^{60}Co spectra. The simplest is the frequently used approximation that ^{60}Co is a single line at 1.25 MeV. The next simplest is to consider ^{60}Co as if from a bare source, viz., two equiprobable photon lines at 1.175 and 1.334 MeV. The next spectrum used is that published in 1988 for a broad ^{60}Co beam.[26] This spectrum has been widely used for Monte Carlo calculations since it is distributed with the EGS4 and EGSnrc systems. The final two spectra are those calculated by Mora *et al.*[27] for NRC's Eldorado 6 ^{60}Co unit. They are the central-axis spectra at a SSD of 80 cm for 10×10 and 30×30 cm^2 fields. For all other calculations reported in this work we use the Mora *et al.* spectra for the 10×10 cm^2 field since this is what applies at NRC. In the previous work of Rogers and Treurniet,[13] the 1988 spectrum was used.

Figure 5 shows that there is a non-negligible, 0.1%, variation in K_{wall} as one changes from the bare source spectrum to the more realistic spectra. However, the variation in K_{wall} for the different realistic ^{60}Co spectra is negligible (0.02%). This implies that K_{wall} calculations can be done with any reasonably realistic ^{60}Co spectrum.

Figure 6 shows that the variation of calculated K_{an} values with incident spectrum is not large, but in this case the statistical uncertainties are greater. Whatever the variation, it is unlikely to be greater than 0.07%.

Figure 7 shows the variation in the calculated stopping-power ratio for different incident ^{60}Co spectra. There is more than a 0.13% change between using a realistic spectrum versus using monoenergetic or near-monoenergetic spectra, but less than 0.03% variation between the values for different realistic spectra.

V. VARIATION WITH SOURCE DIAMETER

In the past, all calculations using CAVRZ or CAVRZnrc have modeled sources as parallel beams or as point sources at an arbitrary distance and angle. However, actual ^{60}Co sources are cylindrical in shape, with the flat surface towards the calibration point having a radius of 1 cm or more. To investigate the effect of this finite size, a series of calculations was done with a new source routine which allows for a uniform circular or square source perpendicular to the line

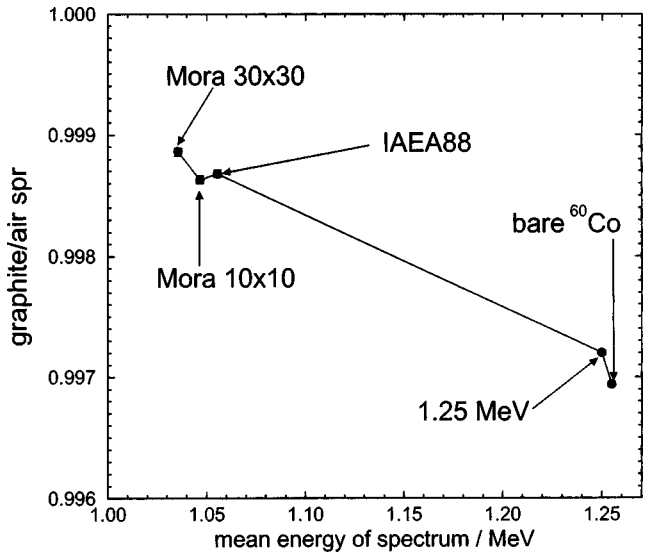

FIG. 7. Variation of ^{60}Co graphite to air stopping-power ratio with the spectrum incident on the phantom. These results are done with regeneration on a 1.5 cm phantom. The graphite density effect is for a density of 2.265 g/cm^3 and the value of Δ is 19 keV.

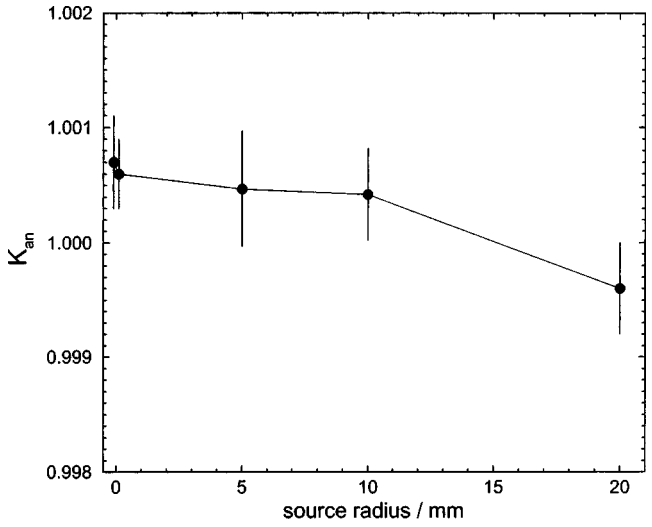

FIG. 8. Variation of K_{an} value for the 3C chamber as the assumed size of the ^{60}Co source is increased. Two calculations for the point source case were done using two different source routines and are shown slightly offset for clarity.

joining the source to the ion chamber. The variation in K_{wall} values as the source radius is increased from 0 to 20 mm is less than 0.01%.

Figure 8 shows the variation in the calculated value of K_{an} as the source radius is increased. In this case there appears to be a slight variation, especially for the largest size, but it is not statistically significant. In any event, out to the actual size of the source at NRC (about 10 mm radius), the variation is negligible within the 0.04% statistics.

VI. EFFECTS ON K_{wall} OF DISTANCE FROM A POINT SOURCE

Figure 9 shows the variation in K_{wall} values for the NRC 3C chamber as the source distance is varied. There is more than a 0.1% decrease in K_{wall} going from a parallel beam to a point source at 100 cm and a further 0.06% decrease as the distance drops to 50 cm. There is obviously no uncertainty in K_{wall} due to the distance uncertainty. However, the calculations must be done for a point source at the appropriate source-detector distance rather than for a parallel beam incident (as done previously at NRC).

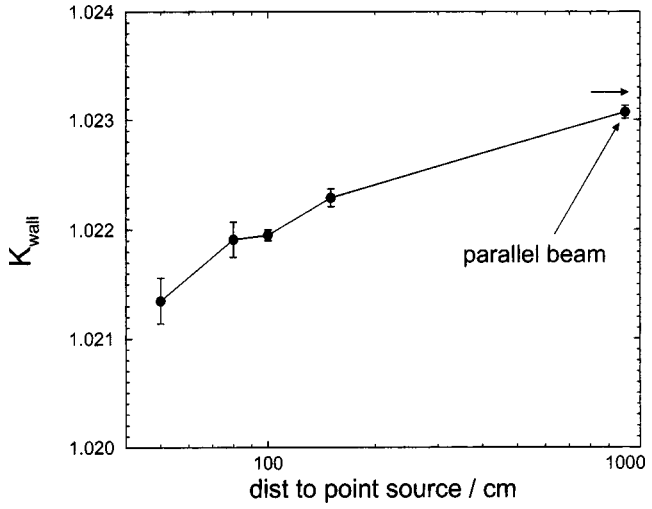

FIG. 9. Variation of K_{wall} value for the 3C chamber as a function of distance from a point source.

There is no corresponding uncertainty in the stopping-power ratio since it is calculated for a parallel beam as required by the theory.

VII. THE K_{comp} CORRECTION FOR THE INSULATOR

As noted when Fig. 1 was presented, the 3C chamber has a rather large polystyrene insulator. Borg *et al.*[6] noted that this insulator leads to a decrease of 0.4% in the ion chamber response and thus the K_{comp} correction factor in Eq. (1) has a value of 1.004.

The K_{comp} correction is defined by Eq. (3). It is slightly different from the definition of Borg *et al.* where the quantities were for a point source rather than a parallel beam.

We recalculate K_{comp} using Eq. (3) and the latest version of EGSnrc, with stopping powers for graphite reflecting the grain density in the density effect and the ^{60}Co spectrum for a 10×10 cm^2 ^{60}Co beam rather than the 35×35 cm^2 spectrum used previously. We find $K_{comp}=1.0046(3)$ which is consistent with, but more accurate than, the previous calculation. Only 0.02% of the change is related to the change in definition. For interest we also calculated $(K_{wall})_{graphite}/(K_{wall})_{realistic}$ for a parallel beam and find it is 0.07(1)% greater than unity, i.e., the insulator has only a small effect on the value of K_{wall}.

VIII. CALCULATION OF STOPPING-POWER RATIOS

VIII. A. Effects of phantom size on stopping-power ratios

Stopping power ratios are calculated essentially by scoring the electron fluence spectrum in a phantom made of the wall material (i.e., there is no cavity involved in the calculations). Since there is a phantom, the electron fluence spectrum will vary with location, with lack of full buildup near the surface and with photon scatter and attenuation affecting the electron distribution differently at various points in the phantom. This introduces a phantom-size dependence into the calculation of stopping-power ratios.

To investigate this effect, we calculate the stopping-power ratio in the central portion of a small cylindrical graphite phantom with differing amounts of buildup around the central core where the electron fluence is scored. The solid line in Fig. 10 shows that the stopping-power ratio increases by 0.2% going from a mini-phantom with a core radius and outer buildup region of 0.5 mm to a mini-phantom with a core radius and outer buildup region of 1 cm. The photon attenuation and scatter in the phantom are included in these calculations. If this were the correct method, there would be a problem due to this phantom-size dependence since it does

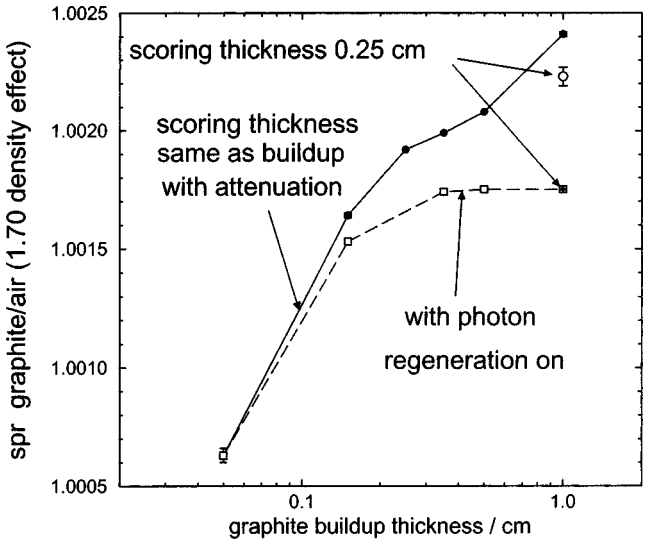

FIG. 10. Variation of ^{60}Co graphite to air stopping-power ratio with the thickness of the buildup layer in the graphite cylindrical mini-phantom used to score the electron spectrum. The graphite density effect used in the calculations assumes a graphite density of 1.70 g/cm^3 and the value of Δ is 10 keV. The scoring region is the same thickness as the surrounding buildup region except for the two additional data points with 1 cm buildup, for which the scoring region is only 0.25 cm across. For the solid line, photon attenuation and scatter occur whereas for the dashed line photon attenuation and scatter are turned off in the calculation, thereby making the calculated value independent of the geometry once full buildup is achieved.

not reach an equilibrium. However, as Borg *et al.*[6] pointed out, this is not the correct method since the underlying theory requires that attenuation and scatter in the phantom be excluded from the calculation. Turning on the so-called regeneration option in CAVRZnrc, one obtains the curve shown by the dashed line in Fig. 10. There is still considerable variation prior to full buildup being achieved in the mini-phantom, but once this is achieved the calculated stopping-power ratio becomes constant.

Thus, as long as the photon regeneration option is used and the phantom is large enough to ensure full buildup in the scoring region, there is no uncertainty nor ambiguity in the stopping-power ratio due to the size of the phantom.

VIII. B. Selecting values of Δ

Although the definition of Δ is not conceptually rigorous,[28] it is usually taken as the energy of an electron which would have a residual range in air which was equal to L, the mean chord length of electrons in the cavity of the ion chamber. For isotropic electrons uniformly entering a convex cavity, $L=4V/S$ where V is the volume and S is the surface area.[28] This is the expression used by most standards laboratories to determine the value of Δ appropriate for their standard cavity chambers. However, electrons entering the cavity of an ion chamber are not necessarily isotropic, nor are all ion chambers convex. In particular, NRC's 3C chamber is concave due to its large central electrode.

To investigate the effect of the breakdown of these assumptions, the CAVRZnrc code was modified to score the average chord length of the electrons entering an ion chamber cavity for different incident photon beams. The cavity is treated as a vacuum to ensure straight paths, but otherwise the chamber is as realistic as possible within the cylindrical approximation. Table I presents the results for the chambers of several standards labs using the $4V/S$ formula or the Monte Carlo code. The Monte Carlo calculations are done for an ECUT value of 10 keV (kinetic energy) although calculations for the 3C chamber with an ECUT of 1 keV showed no difference other than taking ten times as long. Table I shows that the simple formula is remarkably accurate, even for the concave 3C chamber. The Monte Carlo code does predict a noticeable variation in Δ as the beam is incident on the front or the side of the NRC Mark IV pancake chamber,[14] but the implied change in the stopping-power ratio is less than 0.05% and is thus negligible.

TABLE I. Values of mean chord length and corresponding Δ values as calculated using the formula $L=4V/S$ or the Monte Carlo code (for a ^{60}Co beam although for 100 keV photons the results are very similar). Values of Δ are the energies of an electron having a residual CSDA range of L using the range data in ICRU Report 37.[29] No correction for path curvature is included although this is sometimes done. Dimensions for the BIPM pancake chamber and widely used OMH cylindrical chamber are taken from Ref. 13.

	$4V/S$		Monte Carlo	
Chamber	L (mm)	Δ (keV)	L (mm)	Δ (keV)
3C	7.6	19.3	8.0	19.8
Mark IV flat	2.1	9.1	1.8	8.5
Mark IV side	2.1	9.1	2.4	10.1
BIPM pancake	4.0	13.4	3.5	12.4
OMH	6.5	17.6	6.6	17.8
Baldwin–Farmer	4.8	14.8	4.6	14.5

VIII. C. Effects of different density effects and values of I and Δ

Figure 11 presents the values of $(\overline{L}/\rho)_{\text{air}}^{\text{graphite}}$ for a ^{60}Co beam as a function of Δ. The two upper curves were calculated using the density effects presented in ICRU Report 37, one for a typical graphite bulk density of 1.70 g/cm^3, as recommended in ICRU Report 37, and the other with the grain density of graphite, viz., 2.265 g/cm^3. As discussed above, experimental data imply there is a preference for using the grain density in the present calculations. Assuming the standard ICRU mean ionization value for graphite, this implies a 0.23% decrease in the graphite to air stopping-power ratio for the 3C chamber where the appropriate value of Δ, as given by the mean chord length, is 20 keV.

The values of the stopping powers in graphite presented in ICRU Report 37 are based on an I-value in graphite of 78 ± 7 eV[29] (where the uncertainty is roughly at the 90% confidence level), but the most recent and highly accurate measured I-value is 86.8 ± 1.2 eV.[30] Using Berger's ESTAR program,[31] which was used to generate the values in ICRU Report 37, we calculate stopping-power ratios using an I-value of 87 eV and a density of 2.265 g/cm^3 for the density effect. The corresponding stopping-power ratios are the third curve in Fig. 11. For $\Delta=20$ keV, these values show a dra-

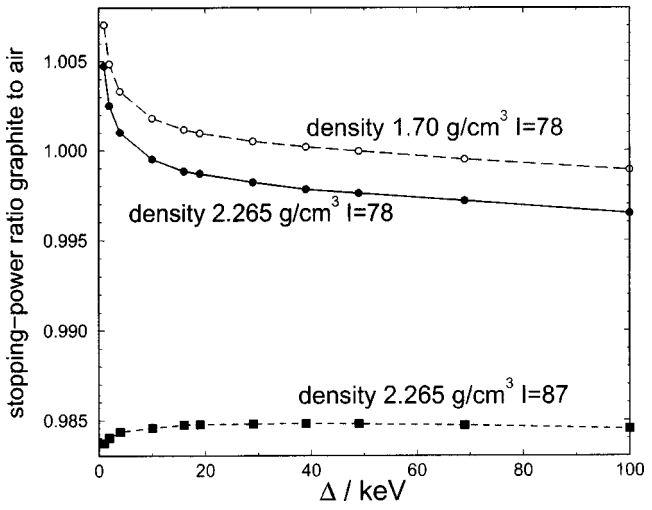

FIG. 11. Variation of ^{60}Co graphite to air stopping-power ratio with Δ, the low-energy transport cutoff used in the calculations corresponding to the mean chord length of particle tracks in the chamber. The upper two sets of calculations were done with stopping powers from ICRU Report 37 for two different density effects. The lower curve uses stopping powers calculated using the same program as used to generate values in ICRU Report 37, but for a graphite I-value of 86.8 eV. Photon regeneration was on for these calculations which were done in a mini-phantom with 5 mm of buildup and using the 10×10 cm^2 ^{60}Co spectrum of Mora *et al.*[27]

matic decrease of nearly 1.6% compared to the standard curve ($I=78,\rho=1.70$ g/cm^3). Since this new I-value for graphite is close to that of air, the variation of the stopping-power ratio as a function of Δ is almost nonexistent for Δ values above 10 keV.

The BIPM's CCRI has agreed that the minimum uncertainty on the graphite to air stopping-power ratio to be used in a ^{60}Co beam is 0.7%. The change of 0.23% resulting from the density effect is well within this uncertainty, but the 1.6% change from the I-value is not. In principle this adjustment in stopping-power ratio is not relevant because what enters into the calculations for the primary standards is the product $(W/e)_{\rm air}(\overline{L}/\rho)^{\rm graphite}_{\rm air}$ and this product has a much smaller uncertainty. However, in practice what most NMIs appear to do is multiply the recommended value of $(W/e)_{\rm air}$ by the appropriate value of $(\overline{L}/\rho)^{\rm graphite}_{\rm air}$ for their chamber. This is incorrect if a new stopping power is used unless a complete reanalysis is done to determine the appropriate value of $(W/e)_{\rm air}$ corresponding to the new value of $(\overline{L}/\rho)^{\rm graphite}_{\rm air}$ being used in the rest of the analysis. A better approach would be to adopt a standard value for the product $(W/e)_{\rm air}(\overline{L}/\rho)^{\rm graphite}_{\rm air}$ with corrections, if needed, for the variations due to different cavity sizes. In the absence of such a complete reanalysis, we will just use the accepted value of $(W/e)_{\rm air}$ and our best estimate of $(\overline{L}/\rho)^{\rm graphite}_{\rm air}$. This is not correct in principle, but moves the product in a direction consistent with the values suggested by a detailed but still preliminary reanalysis.[32]

IX. THE RADIATIVE CORRECTION, $\bar{g}$

Equation 1 requires a value of $\overline{g}_{\rm air}$, the fraction of the energy transferred by a ^{60}Co beam to electrons in air which is lost via radiative events. Borg *et al.*[6] have calculated a value of $\overline{g}_{\rm air}=0.31\%$ based on an EGSnrc Monte Carlo calculation using ICRU Report 37's radiative stopping powers and a realistic ^{60}Co spectrum. This is in good agreement with the previously used value of 0.32%.[18,33]

TABLE II. Summary of the proposed changes to the Canadian primary standard for air kerma based on the current Monte Carlo calculations.

Quantity	1990 value	Present value	% Change
$\left(\frac{\overline{L}}{\rho}\right)^{\rm graphite}_{\rm air}$	1.0005	0.9987	−0.18%[a]
		1.0010	+0.05%[b]
$K_{\rm wall}$	1.0218	1.0220	+0.02%[c]
$1.0-\overline{g}$	0.9968	0.9969	+0.01%
$K_{\rm comp}$	1.000	1.0046(3)	+0.46%
$K_{\rm an}$	0.9999(6)	1.0004(4)	+0.05%
Overall change: with sp[d] change: +0.31% without sp[d] change: +0.54%			

[a] −0.23% from change in density effect, +0.14% from change in spectrum −0.07% going to $\Delta=19$ keV, +0.02% from using EGSnrc and −0.04% from using regeneration.
[b] as in[a] but with no change in the stopping power used.
[c] −0.08% using a spectrum, +0.12% using a point source, −0.02% using EGSnrc.
[d] sp = stopping power. The change referred to is from changing density effects.

X. CHANGES TO THE CANADIAN AIR-KERMA STANDARD

Table II presents a summary of the changes needed in the Canadian primary standards of air kerma based on the above calculations.

X. A. Stopping-power ratio

The NRC primary standard of air kerma in a ^{60}Co beam, as declared in 1990, uses a value of $(\overline{L}/\rho)^{\rm graphite}_{\rm air}=1.0005$ (Ref. 33) based on a density effect corresponding to a graphite density of 1.70 g/cm^3, a Δ value of 10 keV, and a monoenergetic 1.25 MeV photon beam.

The current best estimate of the stopping-power ratio for the NRC 3C primary standard is 0.9987 based on using the EGSnrc user-code SPRRZnrc with regeneration, a value of Δ of 20 keV, a density effect based on $\rho=2.265$ g/cm^3, an I-value of 78 eV, and the realistic ^{60}Co spectrum of Mora *et al.*[27] If we use the recommended density effect, viz., that based on $\rho=1.70$ g/cm^3, the value is 1.0010.

Figure 7 implies that using the 1.25 MeV approximation makes the previous value 0.14% low compared to the value calculated with the more realistic spectrum for a 10×10 cm^2 field. Figure 4 suggests the previous value was 0.02% low as a result of using EGS4/PRESTA. Figure 10 suggests that the previous value may have been 0.04% high because the SPRRZ code did not use photon regeneration (see Sec. VIII A). Figure 11 implies the previous value was 0.07% high because it was for a value of $\Delta=10$ keV rather than the 20 keV value appropriate for the 3C chamber (see Table I). As discussed in Sec. VIII C, it is now believed that the stopping-power ratio should be based on a density effect for the grain density and this implies a decrease of 0.23%.

In summary, the two ''major'' changes in stopping-power ratio are from using a realistic incident spectrum for the simulations and from the change in the density effect used. Fortunately, these effects offset each other and the overall change is a decrease of 0.18%. Ignoring the change in the stopping power, the other changes lead to an increase of only 0.05%.

X. B. K_{wall}, K_{comp}, and K_{an}

The value of K_{wall} used in 1990 was 1.0218 and the current best estimate is 1.0220, i.e., an increase of 0.02%. Figure 5 implies that using a realistic spectrum instead of 1.25 MeV incident photons decreases K_{wall} by 0.08% and Fig. 9 implies a 0.12% increase because of using a point source rather than a parallel beam. Figure 3 suggests a 0.02% decrease from using EGSnrc instead of EGS4/PRESTA. Again the changes cancel almost exactly.

Although Henry estimated $K_{comp}=1.002$,[18] this effect was not included in the 1990 revision and hence the current estimate of 1.0046 represents a 0.46% increase.

The value used in 1990 for the correction K_{an} was 0.9999(6) based on Bielajew's analytic theory.[9] The current estimate, based on the Monte Carlo calculations, reported here for a source of radius 1 cm at 100 cm is 1.0004(4), which is consistent with the previous value.

XI. UNCERTAINTY ESTIMATES

Uncertainty estimates for each of these factors are needed as part of the uncertainty budget for primary standards for air kerma. As discussed in Sec. VIII C, the uncertainty on the stopping-power ratio itself does not enter into this budget because one really needs the uncertainty on the product $(W/e)_{air}(\overline{L}/\rho)_{air}^{graphite}$. Nonetheless, here we will assess the uncertainty on the stopping-power ratio itself since this is needed for other applications such as the analysis of the mean value of $(W/e)_{air}$.

The simplest component of the uncertainty to deal with is the Monte Carlo statistical uncertainty on each factor. It varies from 0.01% or less for the stopping-power ratio and K_{wall}, to 0.04% and 0.03% for K_{an} and K_{comp}, respectively.

A more complex component is the uncertainty associated with the algorithm used in the Monte Carlo code. Figure 4 suggests that the uncertainty on the stopping-power ratio is 0.01% or less using various options with EGSnrc, and not much more if one uses EGS4/PRESTA. For K_{wall}, Fig. 3 implies that the uncertainty due to the algorithm is no more than 0.02%. In both cases, a relatively small uncertainty results because the factors are based on ratios of dose calculations. This also applies to both K_{comp} and K_{an} which have much poorer statistical precision. We therefore adopt the same 0.02% for these factors without repeating the same calculations.

The uncertainty due to the incident beam used in the calculations can be estimated from Figs. 5, 6, and 7 for K_{wall}, K_{an}, and $(\overline{L}/\rho)_{air}^{graphite}$, respectively, by examining the variation in the values for the three realistic spectra. This leads to uncertainties of 0.01%, 0.07%, and 0.02%, respectively. Similar calculations for realistic spectra imply an uncertainty of 0.07% on the value of K_{comp}. These are conservative estimates since they represent the range of values calculated and thus apply for generic calculations using an arbitrary realistic spectrum. The uncertainty when using a spectrum calculated for the specific unit being used is taken as half of the range for each factor.

Figure 8 and similar calculations for K_{wall} suggest uncertainties due to the source radius dependence of 0.01% and 0.02% for K_{wall} and K_{an}, respectively. The effect of source radius on other factors is expected to be negligible.

There is some uncertainty in the stopping-power ratio on account of the lack of a precise definition of Δ. Figure 11 suggests an uncertainty of 0.05% if the uncertainty in the value of Δ is 7 keV, which is an arbitrary, but conservative, estimate. This same figure implies that if an I-value of 87 eV is adopted for graphite, then the value of the stopping-power ratio is independent of the value of Δ.

The most complex and largest part of the uncertainty in each factor comes from the uncertainty in the underlying photon and electron cross-sections.

For the uncertainty on the stopping-power ratio we follow the approach used in Ref. 34 but introduce the ability to calculate ICRU equivalent stopping powers based on the NIST program ESTAR[31] and incorporate new knowledge about the appropriate density effect correction.

It is difficult to assign an uncertainty related to the choice of which density effect to use. In accordance with a CCRI recommendation, we use the 1.70 g/cm^3 density effect and yet the best evidence to date suggests we should use the grain density effect which leads to a 0.23% decrease in the stopping-power ratio (see Fig. 11). Typically one might average the two values and take half the difference as the uncertainty. This cannot be done here since the value used is that adopted by agreement, so we choose to adopt an uncertainty corresponding to the full difference between the two options.

The same argument could be applied to the possibility of using the new I-value for graphite which would lead to a further decrease of 1.4% which seems too large. Instead we have considered the effect of changing the graphite I-value from 78 eV by 3.5 eV, the ICRU's best estimate of a one standard deviation uncertainty on the I-value for graphite.[29] Changing the graphite I-value by 3.5 eV and using a density of 1.70 g/cm^3 we get an increase in the stopping-power ratio of 0.59%. Similarly, the ICRU uncertainty on the I-value of air (85.7 eV) is 1.7 eV (ICRU's table 5.6, 90% confidence) or 0.8 eV (68% confidence), which leads to a decrease of 0.13% in the stopping-power ratio.

Summing these last three uncertainties in quadrature gives an overall uncertainty of 0.65% in the stopping-power ratio due to the uncertainties in the I-value and the density to use when calculating the density effect for the stopping powers. This ignores the uncertainty in the theory and methods used to calculate the stopping power, but we will assume these are small compared to the uncertainties already mentioned.

Following the same general approach, if we use a graphite stopping power with $I=74.5$ eV during the calculation of the

K_{comp} correction, the overall response of the chamber is found to increase by 0.7% (as expected based on the 0.6% decrease in the stopping-power ratio mentioned above), but the change in the value of K_{comp} itself is only $0.06 \pm 0.06\%$, a reflection of the small change in the calculated responses due to the differences between graphite and polystyrene. Including the uncertainties concerning which density effect to use for graphite and the uncertainty in the polystyrene stopping power leads to an overall uncertainty of 0.08% in K_{comp} due to the uncertainty in the stopping powers.

The values of K_{wall} and K_{an} are insensitive to the electron stopping powers since they are ratios of calculated doses. This was confirmed when only a statistically insignificant change of 0.01% in K_{wall} was observed during an investigation of the K_{comp} uncertainty mentioned above.

The uncertainties in these factors resulting from the photon cross-section uncertainty (about 1%) are less significant because almost all factors are ratios of calculations. Thus, in principle the stopping-power ratio and the value of K_{an} are independent of any reasonable change in the photon cross-section. The values of K_{wall} and K_{comp} are in principle sensitive to uncertainties in the photon cross-section. Mainegra-Hing *et al.*[5] have studied the sensitivity of K_{wall} to the uncertainty in photon cross-sections and shown it to be very small: a 1% change in the photon cross-sections yields less than a 0.01% change in the calculated value of K_{wall} for the Canadian standard 3C chamber. Similarly, a worst case 1% increase in the photon cross-section of one material and a corresponding 1% decrease in the other (graphite and polystyrene) leads to a 0.14% change in the calculated value of K_{comp}. In the K_{wall} case this lack of dependence on the cross-section can be understood in the sense that the increase or decrease in the attenuation is always made up for by a compensating decrease or increase in the scatter, and these nearly cancel. In the case of K_{comp}, one must recognize that it is only the 0.5% composite wall effect that is sensitive, more or less directly, to the cross-sections. Thus the 1% uncertainty in the cross-sections has a much reduced effect on the correction factor itself.

Table III summarizes the uncertainties on these factors. The uncertainty in the underlying cross-sections dominates the uncertainty in the stopping-power ratio and K_{comp}. The remainder of the uncertainties are very small. Note also that the current analysis is very conservative since correlations between the various quantities are ignored. It is possible to write

$$K_3 = (D_{gas} K_{wall})^{\text{graphite,parallel}} / D_{gas}^{\text{realistic,point}}, \tag{5}$$

where K_3 replaces the product $K_{wall}K_{an}K_{comp}$. Doing this calculation would reduce the uncertainties somewhat, in particular, reducing the statistical uncertainty for the same computing time. One could go one step further and calculate an overall correction factor, replacing Eq. (4) with

$$K_{air} = \frac{D_{gas}}{(1-\overline{g}_{wall})} \left(\frac{\overline{\mu_{tr}}}{\rho} \right)_{wall}^{air} K_{overall} \quad \text{(Gy)}, \tag{6}$$

TABLE III. Summary of uncertainties in calculated factors. All values are in %. The uncertainty on the product assumes the factors are independent, which is an overly conservative assumption. An uncertainty of 0.07% reflecting the accuracy of the Spencer–Attix theory without a fluence correction factor is not included (see Sec. XI).

Effect	$\left(\frac{\overline{L}}{\rho}\right)_{air}^{graphite}$	K_{wall}	K_{an}	K_{comp}	Product
statistics	<0.01	<0.01	0.04	0.03	
algorithm	0.02	0.02	0.02	0.02	
spectrum	0.01	<0.01	0.04	0.04	
source size	⋯	0.01	0.02	⋯	
distance	⋯	0.01	⋯	⋯	
Δ selection	0.05	⋯	⋯	⋯	
Subtotals	0.05	0.03	0.06	0.05	0.10
cross-sections					
electron	0.65	0.01	⋯	0.08	
photon	⋯	0.01	⋯	0.14	
Totals	0.65	0.03	0.06	0.17	0.67

where D_{gas} is calculated for a point source incident on the realistic model of the 3C chamber. Solving this for $K_{overall}$ and using the fact that $K_{med} = (\overline{\mu_{tr}}/\rho)_{med}$ (since all absolute quantities are normalized per unit photon fluence) gives

$$K_{overall} = \frac{(\overline{\mu_{tr}}/\rho)_{wall}(1-\overline{g}_{wall})}{D_{gas}} = \frac{(\overline{\mu_{en}}/\rho)_{wall}}{D_{gas}}, \tag{7}$$

from which we get $K_{overall} = 1.0269$ which is 0.13% lower than the value 1.0282 determined as the product $K_{wall}K_{an}K_{comp}(\overline{L}/\rho)_{air}^{graphite}$. One might expect that the calculated value of $K_{overall}$ would have a smaller uncertainty than the product of the four factors. However, calculating $K_{overall}$ requires the absolute calculation of the dose in the chamber cavity and this quantity is subject to the 0.1% systematic uncertainty in this EGSnrc calculation[24] (ignoring uncertainties from the cross-sections). As shown above, this uncertainty does not apply to the various correction factors since they involve ratios of dose calculations, and these are subject to smaller uncertainties. In the comparison there is also the uncertainty in the Spencer–Attix theory as applied here. In particular, no account has been taken of a possible fluence correction factor which might be of the order of 0.07% as suggested by the results of Borg *et al.* for the 3C chamber with pure graphite walls[6] and of Mainegra-Hing *et al.*[5] for plane-parallel chambers (although these were conservative estimates since there is a comparable uncertainty in the accuracy of the calculations). This uncertainty exists in both approaches: it enters directly into the calculation of the uncertainty on $K_{overall}$, whereas when applying the individual corrections, it is just an overall uncertainty in the application of Spencer–Attix cavity theory without a fluence correction factor.

Given the 0.10% uncertainty on the product given in Table III and the above observations, the 0.13% difference between $K_{overall}$ and the product of the four correction factors is not surprising.

Although the calculation of $K_{overall}$ is equivalent to the approach taken in this article, it breaks with the traditional concept of a correction factor and we will not use it.

XII. DISCUSSION

These results impact directly on an argument in a recent paper[15] where it was argued that the near unity value (1.001 ± 0.004)[35] for the ratio of the Canadian air-kerma standard (which uses a calculated value of K_{wall}) and the French standard (which bases its ''measured'' value of K_{wall} on Bielajew's model[15]) gives ''an indirect indication that the Bielajew model and the Monte Carlo technique give consistent values for the wall correction factor.'' With the recognition that the NRC standard should be increased by 0.54%, the previously good agreement becomes less satisfactory, viz., $0.995_6 \pm 0.004$. The problem may lie in the methods used by the French laboratory to determine K_{wall}. The value they use is 1.0152 ± 0.0021,[36] whereas the Monte Carlo calculated value for their chamber is between 1.0244 and 1.0241 (the chamber is a cylinder with two spherical ends and the two values are for cylindrical and spherical models of the chamber, respectively).[13] If we were to use the Monte Carlo calculated K_{wall} value of 1.0243 for the French standard, the result of the comparison, after correcting the NRC standard by 0.54%, would be 1.004_5. This is still not as satisfactory as the original result. In any event, the previous close agreement does not tell us much about the accuracy of the particular models used to determine K_{wall}.

XIII. SUMMARY AND CONCLUSIONS

The calculations presented here demonstrate that values of the correction factors needed for primary standards of air kerma can be reliably calculated using Monte Carlo. This work presents the first systematic effort to assign realistic uncertainties to many of these calculated factors. The sensitivity to various calculation algorithms has been explored and shown not to be a significant issue.

It has been shown that primary standards of air kerma in a ^{60}Co beam are sensitive to the parameters used for the graphite stopping powers. Given all the other changes currently taking place in the field (related to the corrections K_{wall}, K_{comp}, and K_{an}), this would be a good time to make a change in the stopping powers adopted for graphite. Based on the measured results for higher energy electrons,[22,23] it seems clear that the grain density should be used, which leads to a 0.23% decrease in the Canadian standard. If one were to further adopt the new I-value for graphite based on the measurements of Bichsel and Hiraoka,[30] this would lead to an additional 1.39% decrease in the Canadian (and all other similar) standards. Such a change usually occurs by consensus agreement between the standards laboratories.

It has been shown that the calculated stopping-power ratios are insensitive to which algorithm is used to calculate them and only slightly sensitive to the ^{60}Co spectrum used (0.03% variation between three realistic spectra) although calculations based on a simple 1.25 MeV incident beam of photons are low by about 0.16%.

Aside from the stopping-power ratios, the other major change in the Canadian standard is the introduction of a new value for K_{comp}. The polystyrene insulator leads to a 0.46% correction for the 3C chamber.

Studies have shown that K_{wall} must be calculated using a realistic spectrum for the ^{60}Co beam, but the details are not critical provided a mono-energetic beam is not used. Similarly, it is important to do the calculations for roughly the correct source distance, but this is not critical as long as a parallel-beam configuration is avoided. The K_{wall} values are completely insensitive to the radius assumed for the ^{60}Co source.

The values of K_{an} do not depend significantly on the spectrum used for their calculation and there is only a slight (barely significant for reasonable radii) dependence on the assumed source radius.

The overall increase in the Canadian primary standard for air kerma based on these Monte Carlo calculations is 0.54%. Given the many changes being made in other primary standards as they adopt calculated values of K_{wall} and K_{an} for some laboratories (average increase expected is 0.8%), the change in the Canadian standard will only prevent Canada from becoming an outlier since we already have been using calculated values for K_{wall} and K_{an}. An in-depth reevaluation of previous comparisons will be made once the other standards have been changed.

NRC intends to adjust its standard in the near future to reflect the changes in the correction factors used, but clients will be formally notified when this occurs. Any changes based on changes in electron stopping-power values will likely await a CCRI/standards-laboratories decision to make a change in the recommended values.

ACKNOWLEDGMENTS

We wish to thank our colleagues John McCaffrey and Ken Shortt for extensive discussions about the Canadian primary standard and the various correction factors involved. Our thanks also to Michel Proulx, Blake Walters and Ernesto Mainegra-Hing for support of the EGSnrc Monte Carlo system, upon which this study is based. Thanks also to Pat Saull, Malcolm McEwen, and Carl Ross for helpful comments on the manuscript.

[a]Electronic mail: dave@irs.phy.nrc.ca

[1] AAPM TG-21, ''A protocol for the determination of absorbed dose from high-energy photon and electron beams,'' Med. Phys. **10**, 741–771 (1983).

[2] IAEA, *Absorbed Dose Determination in Photon and Electron Beams; An International Code of Practice*, Vol. 277 of Technical Report Series (IAEA, Vienna, 1987).

[3] P. R. Almond, P. J. Biggs, B. M. Coursey, W. F. Hanson, M. S. Huq, R. Nath, and D. W. O. Rogers, ''AAPM's TG-51 protocol for clinical reference dosimetry of high-energy photon and electron beams,'' Med. Phys. **26**, 1847–1870 (1999).

[4] D. W. O. Rogers and C. K. Ross, ''The role of humidity and other correction factors in the AAPM TG-21 dosimetry protocol,'' Med. Phys. **15**, 40–48 (1988).

[5] E. Mainegra-Hing, I. Kawrakow, and D. W. O. Rogers, ''Calculations for plane-parallel ion chambers in ^{60}Co beams using the EGSnrc Monte Carlo code,'' Med. Phys. **30**, 179–189 (2003).

[6] J. Borg, I. Kawrakow, D. W. O. Rogers, and J. P. Seuntjens, "Monte Carlo study of correction factors for Spencer-Attix cavity theory at photon energies at or above 100 keV," Med. Phys. **27**, 1804–1813 (2000).
[7] D. W. O. Rogers and A. F. Bielajew, "Wall attenuation and scatter corrections for ion chambers: measurements versus calculations," Phys. Med. Biol. **35**, 1065–1078 (1990).
[8] A. F. Bielajew, "On the technique of extrapolation to obtain wall correction factors for ion chambers irradiated by photon beams," Med. Phys. **17**, 583–587 (1990).
[9] A. F. Bielajew, "An analytic theory of the point-source non-uniformity correction factor for thick-walled ionisation chambers in photon beams," Phys. Med. Biol. **35**, 517–538 (1990).
[10] A. F. Bielajew and D. W. O. Rogers, "Implications of new correction factors on primary air kerma standards in ^{60}Co beams," Phys. Med. Biol. **37**, 1283–1291 (1992).
[11] I. Kawrakow and D. W. O. Rogers, "The EGSnrc Code System: Monte Carlo simulation of electron and photon transport," Technical Report PIRS-701, National Research Council of Canada, Ottawa, Canada, 2000.
[12] W. R. Nelson, H. Hirayama, and D. W. O. Rogers, "The EGS4 Code System," Report SLAC-265, Stanford Linear Accelerator Center, Stanford, CA, 1985.
[13] D. W. O. Rogers and J. Treurniet, "Monte Carlo calculated wall and axial non-uniformity corrections for primary standards of air kerma," NRC Report PIRS-663, NRC, Ottawa, 1999 (see http://www.irs.inms.nrc.ca/inms/irs/papers/PIRS663/pirs663.html).
[14] J. P. McCaffrey, K. R. Shortt, I. Kawrakow, and D. W. O. Rogers, "Wall attenuation and scatter corrections for ion chambers," in *Proc. of 2001 COMP Annual Meeting* (Canadian Organization of Medical Physicists, Edmonton, Alberta, 2001), pp. 79–81.
[15] K. R. Shortt, A. F. Bielajew, C. K. Ross, K. J. Stewart, J. T. Burke, and M. J. Corsten, "The effect of wall thickness on the response of a spherical ionization chamber," Phys. Med. Biol. **47**, 1721–1731 (2002).
[16] R. F. Laitano, M. P. Toni, M. Pimpinella, and M. Bovi, "Determination of K_{wall} correction factor for a cylindrical ionization chamber to measure air-kerma in ^{60}Co gamma beams," Phys. Med. Biol. **47**, 2411–2431 (2002).
[17] L. Büermann, H. M. Kramer, and I. Csete, "Results supporting calculated wall correction factors for cavity chambers," in preparation (2003).
[18] K. R. Shortt and C. K. Ross, "The Canadian ^{60}Co Exposure Standard," National Research Council of Canada Report PIRS-0052 (1986).
[19] I. Kawrakow, "Accurate condensed history Monte Carlo simulation of electron transport. I. EGSnrc, the new EGS4 version," Med. Phys. **27**, 485–498 (2000).
[20] D. W. O. Rogers, I. Kawrakow, J. P. Seuntjens, and B. R. B. Walters, "NRC User Codes for EGSnrc," Technical Report PIRS-702, National Research Council of Canada, Ottawa, Canada, 2000.
[21] A. F. Bielajew and D. W. O. Rogers, "PRESTA: The Parameter Reduced Electron-Step Transport Algorithm for electron Monte Carlo transport," Nucl. Instrum. Methods Phys. Res. B **18**, 165–181 (1987).
[22] M. S. MacPherson, C. K. Ross, and D. W. O. Rogers, "Measured electron stopping powers for elemental absorbers," Med. Phys. **23**, 797 (1996) (abs).
[23] M. S. MacPherson, "Accurate Measurements of the Collision Stopping Powers for 5 to 30 MeV Electrons," Ph.D. thesis, NRC Report PIRS 626, 1998.
[24] I. Kawrakow, "Accurate condensed history Monte Carlo simulation of electron transport II. Application to ion chamber response simulations," Med. Phys. **27**, 499–513 (2000).
[25] B. R. B. Walters, J. Treurniet, D. W. O. Rogers, and I. Kawrakow, "QA tests and comparisons of the EGSnrc system with EGS4," Technical Report PIRS-703, National Research Council of Canada, Ottawa, Canada, 2000.
[26] D. W. O. Rogers, G. M. Ewart, A. F. Bielajew, and G. van Dyk, "Calculation of electron contamination in a ^{60}Co therapy beam," in *Proceedings of the IAEA International Symposium on Dosimetry in Radiotherapy* (IAEA, Vienna, 1988), Vol 1, pp. 303–312.
[27] G. Mora, A. Maio, and D. W. O. Rogers, "Monte Carlo simulation of a typical ^{60}Co therapy source," Med. Phys. **26**, 2494–2502 (1999).
[28] F. H. Attix, *Introduction to Radiological Physics and Radiation Dosimetry* (Wiley, New York, 1986).
[29] ICRU, "Stopping powers for electrons and positrons," ICRU Report 37, ICRU, Washington DC, 1984.
[30] H. Bichsel and T. Hiraoka, "Energy loss of 70 MeV protons in elements," Nucl. Instrum. Methods Phys. Res. B **66**, 345–351 (1992).
[31] M. J. Berger, "ESTAR, PSTAR and ASTAR: Computer Programs for Calculating Stopping-Power and Ranges for Electrons, Protons, and Helium Ions," NIST Report NISTIR-4999 (Washington, DC), available online at http://physics.nist.gov/Star (1992).
[32] D. W. O. Rogers, "Re-evaluation of (W/e) and (W/e) $s_{gr,air}$: Status Report to CCEMRI(I) Meeting," BIPM, April 1995, BIPM document CCEMRI(I)/95-34 (1995).
[33] P. J. Allisy-Roberts, D. T. Burns, K. R. Shortt, and C. K. Ross, "Comparison of the air kerma standards of the NRC and the BIPM for ^{60}Co γ rays," Rapport BIPM-99/12 (2000).
[34] D. W. O. Rogers, "Uncertainties, in the ^{60}Co graphite to air stopping-power ratio and a re-evaluation of $(W/e)_{air}$ values," Report PIRS-363, National Research Council Canada, Ottawa, also BIPM Document CCEMRI(I)/93-28, (1993).
[35] K. R. Shortt, C. K. Ross, J. P. Seuntjens, F. Delaunay, A. Ostrowsky, P. Gross, and E. Leroy, "Comparison of dosimetric standards of Canada and France for Photons at ^{60}Co and higher energies," Phys. Med. Biol. **46**, 2119–2142 (2001).
[36] A.-M. Perroche, M. Boutillon, J. Daures, A. O. F. Delaunay, E. Leroy, and B. Chauvenet, "Comparison of the standards of air kerma and of absorbed dose of the LPRI and the BIPM for ^{60}Co γ rays," BIPM Report BIPM-94/6 (1994).